CHAPTER IV

PERMEATION STUDY OF INDOMETHACIN FROM POLYCARBAZOLE/NATURAL RUBBER BLEND FILM FOR ELECTRIC FIELD CONTROLLED TRANSDERMAL DELIVERY

4.1 Abstract

The transdermal drug delivery system is an alternative route to transport the medical species into the blood system. This method has been continuously developed and improved to overcome limitations and is now suitable for a wide variety of drug molecules. In this work, the influences of electric field and conductive polymer were investigated for developing a unique drug delivery system. Indomethacin, an anti-inflammatory drug, was loaded into polycarbazole (PCz), a conductive polymer, to promote the efficient transportation of the drug. The drug-loaded PCz was blended with natural rubber (NR) to form a transdermal patch. The release and permeation of indomethacin into a phosphate-buffered saline (PBS) buffer (pH 7.4) through PCz/NR film and pig skin was carried out by a modified Franz diffusion cell at the maintained temperature of 37 °C. A UV-visible spectrometer was used to detect the amount of drug released. The drug permeation increased with decreasing crosslink ratio due to more accessible pathways for the drug to diffuse. Moreover, an electric field dramatically improved the diffusion of the drug from the membrane through the pig skin by generating the electrorepulsive force between the anionic drug and the negatively charged electrode. Thus, the PCz/DCNR films are shown here as a potential transdermal patch under applied electric field.

Keywords: Polycarbazole/Natural rubber film/Controlled drug release

4.2 Introduction

Transdermal drug delivery systems (TDDS) are designed to control the delivery of active drugs through a matrix over a period of time after adhering onto the skin (Debjit Bhowmik *et al.*, 2010). These systems avoid the first-pass metabolism and any pain occurred by the mechanical injection. Moreover, TDDS can control the drug levels in blood as occurring in conventional drug delivery systems (Prausnitz and Langer, 2008). A polymer matrix is generally employed to the controlled release system due to the diversity of polymer structures which can be modified to control the release mechanism of the drug molecule (Uhrich *et al.*, 1999).

Natural rubber (*cis*-1, 4-polyisoprene) obtained from *Hevea brasiliensis* has been used as transdermal patches because of its biocompatibility, high mechanical resistance, capability to form a film, and natural stimulant of angiogenesis (Herculano *et al.*, 2010). Natural rubber was fabricated into a film to control the release rate of metronidazole (Herculano *et al.*, 2010), and natural rubber was blended with hydroxypropylmethyl cellulose for preparation of nicotine matrix films (Pichayakorn *et al.*, 2012). However, poor mechanical properties of the rubber occurred by the photodegradation under a strong sunlight (Chou and Huang, 2008), and this effect can be prevented by crosslinking. The UV curing system in the presence of a photoinitiator and a crosslinking agent uses a short time, operates at low temperature, and it efficiently enhances the mechanical properties of natural rubber (Choi *et al.*, 2006).

A conductive polymer can be blended with a natural rubber to provide desirable properties for using in TDDS. Polycarbazole is one of many conductive polymers. It possesses unique electrical, electrochemical, and optical properties (Morin *et al.*, 2005). Polycarbazole is synthesized by the chemical method because of the possibility of bulk synthesis and morphology control (Gupta and Prakash, 2010).

In this work, polycarbazole/natural rubber blend films were prepared by the UV irradiation using trimethylolpropane tris(3-mercaptopropionate) as a crosslinking agent and 2-methyl-4-(methylthio)-2-morpholdino propiophenone as a photoinitiator. The aim of this work is to investigate the electrical and thermal properties,

morphology, and swelling property of drug matrix films. Indomethacin was used as an anionic drug and the release and permeation behaviors of the films were investigated under the effects of degree of crosslinking and electric field strength.

4.3 Experimental

4.3.1 Materials

Carbazole (Cz; Merck), ammonium persulfate (APS; Sigma Aldrich), and hydrochloric acid (HCl, AR; RCI Labscan) acted as a monomer, an oxidizing agent, and a dopant, respectively, were used in the polymerization of polycarbazole. Double-centrifuged natural rubber (DCNR; THAI EASTERN RUBBER CO., LTD.) was successfully utilized to fabricate a DCNR film with Trimethylol-propane tris(3-mercaptopropionate) (TMPTMP; Aldrich), 2-Methyl-4-(methylthio)-2-morpholdino propiophenone (MMMP; Aldrich) acting as a crosslinking agent and a photoinitiator, respectively. Indomethacin (IN; Sigma-Aldrich) was used as an anionic drug. Potassium chloride (KCl), potassium phosphate monobasic (KH_2PO_4), and sodium phosphate dibasic (Na_2HPO_4) were of a biology grade and obtained from Calbiochem. Potassium sodium chloride (NaCl) was purchased from Carlo Erba. All chemicals were employed for the preparation of a phosphate-buffered saline (pH 7.4). Ammonia solution (NH_3; EMSURE), Dichloromethane (DCM, ACS; Burdick& Jackson), hexane (AR; RCI Labscan), hydrogen peroxide (H_2O_2; QRëC), methanol (MeOH, AR; Lobachemie), polyethylene glycol (PEG; Sigma-Aldrich), sodium hydroxide (NaOH, AR; Lobachemie), toluene (AR; QRëC), and distilled water were used as solvents.

4.3.2 Preparation of Indomethacin-loaded Double-centrifuged Natural Rubber Films (IN-loaded DCNR Films)

The crosslinked DCNR was fabricated using UV irradiation in the presence of MMMP as a photoinitiator and TMPTMP as a crosslinking agent according to the procedure of Choi *et al.* (2006). DCNR latex (5 mL, 0.0415 mol) was poured into the TMPTMP/MMMP mixture (mole ratio of TMPTMP: MMMP as 2: 1) at various moles of crosslinking agent at 0.0004, 0.0016, and 0.0032 mol. After homogeneously stirring, the solution of 0.025 g of IN in PEG (2 mL) was added into latex solution and continuously stirred for 30 min. Then, latex was casted on a petri dish and cured under UV irradiation for 5 min.

4.3.3 Synthesis of Polycarbazole (PCz)

PCz was polymerized via the interfacial chemical polymerization according to the method of Gupta and Praksash (2010). Cz monomer (60 mM) in DCM (50 mL) was slowly poured on APS (1.2 M) dissolved in HCl (0.5 M, 50 mL). The solution was left for 7 h. Then, the product was filtered and washed with distilled water and DCM. Then, it was dried at 65 °C for 24 h under vacuum.

4.3.4 Preparation of Indomethacin-doped Polycarbazole (IN-doped PCz)

PCz was dedoped with NH_3 solution (0.1 M). The dedoped PCz and IN were stirred in MeOH (50 mL). The mixture was stirred for 7 h and then filtered. The filtrate was clearly washed with distilled water. The final product was dried in the oven at 65 °C for 24 h.

4.3.5 Preparation of Indomethacin-doped Polycarbazole/ Double-centrifuged Natural Rubber Blend Films (IN-doped PCz/DCNR Films)

IN-doped PCz was added into the latex mixture consisting of DCNR latex, MMMP, TMPTMP, and PEG. The IN-loaded PCz/DCNR mixture was poured on a petri dish and then cured under a UV reactor for 5 min.

4.3.6 Preparation of Pig Skin Membrane

A pig abdominal skin was washed with a normal saline and hair and subcutaneous fat were removed to obtain the thickness of about 0.2 cm. The hairless pigskin was cut into a circle shape with diameter of 1.5 cm and then soaked in PBS buffer of pH 7.4 overnight before the permeation study.

4.3.7 Characterizations

The PCz powder, IN powder, and IN-doped PCz powder were identified for functional groups using the FT-IR spectrometer (Nicolet, Nexus 670). Samples were scanned with 64 scans over a wave number period of 400-4000 cm^{-1}. The powder sample was thoroughly grinded with anhydrous KBr. For the drug matrix films, ATR technique with ZnSe window was applied to investigate functional groups.

Thermogravimetry Differential Thermal Analyzer, TG-DTA, (Perkin Elmer, Pyris Diamond) was used to study the decomposition temperature of PCz and IN-doped PCz. The sample of 5-10 mg was heated from 50 °C to 900 °C under a nitrogen atmosphere at a gas heating rate of 20 °C/min.

Scanning Electron Microscope, SEM, (Hitachi, S4800) was used to investigate the surface morphology of the DCNR films before and after the permeation study. Micrographs of the film were obtained using an acceleration voltage of 15 kV at various magnifications in a range of 200-1000.

A two-point probe meter was used to determine the electrical conductivity by measuring the resistivity of a semiconductor material. It involved only two equally spaced probes which were in contact with a material of unknown resistance. The probes array were placed on the center of the material and connected to a source meter (Keithley, Model 6517A) which provided the applied voltage and the resultant current was recorded. The applied voltage was plotted as a function of the current to determine the linear Ohmic regime for each sample based on the Van der Pauw method. The applied voltage and the current change in the linear Ohmic regime were converted to the electrical conductivity of PCz using Eq.4.1:

$$\sigma = \frac{1}{\rho} = \frac{1}{R_s \times t} = \frac{I}{K \times V \times t} \quad \text{.....(4.1)}$$

where σ is the specific conductivity (S/cm), ρ is the specific resistivity (Ω cm), R_s is the sheet resistivity (Ω), I is the measured current (A), K is the geometric correction factor (3.22×10^{-3}), V is the applied voltage (V), and t is the pellet thickness (cm).

The procedure to determine the swelling and the crosslink density of the crosslinked DCNR films was followed as in ASTM D6814-02. For the determination of swelling, the film immediately weighted after the crosslinking process and calculated following Eq. (4.2) and (4.3):

$$\text{degree of swelling (\%)} = \frac{M_s - M_d}{M_d} \times 100 \quad \text{.....(4.2)}$$

$$\text{weight loss (\%)} = \frac{M_i - M_d}{M_i} \times 100 \quad \text{.....(4.3)}$$

where M is the weight after submersion in the buffer, M_d is the weight after submersion for 72 h, and M_i is the initial weight of the sample.

For studying a crosslink density, the crosslinked DCNR film was cut to 1 cm^2 and weighed in air and MeOH (non-solvent). The square film was immersed in toluene for 5 days to obtain the equilibrium swelling state. Eq. (4.4) was used to calculate the crosslink density (Flory-Rehner equation):

$$\nu_e = \frac{-[\ln(1-V_r) + V_r + \chi_1 V_r^2]}{[V_1(V_r^{1/3} - V_r)/2]} \quad \text{..... (4.4)}$$

where ν_e is the number of chains in a real network per unit volume, V_1 is the molar volume of solvent, V_r is the polymer volume fraction in swollen state, and χ is the Flory interaction parameter of natural rubber.

V_r was calculated following Eq. (4.5):

$$V_r = \frac{\text{Weight of dry rubber} / \text{Density of dry rubber}}{\left(\frac{\text{Weight of dry rubber}}{\text{Density of dry rubber}}\right) + \left(\frac{\text{Weight of solvent absorbed by sample}}{\text{Density of solvent}}\right)} \quad \text{..... (4.5)}$$

and the density of the dry rubber was calculated using the Eq. (4.6):

$$\text{Density at } 23 \pm 2\ ^\circ\text{C (g/mL)} = 0.7913 \times \frac{A}{A-B} \quad \text{.....(4.6)}$$

where A is the weight of specimen measured in air (g), B is the weight of specimen measured in MeOH (g), and 0.7913 is the density of MeOH at 23 ± 2 °C (g/mL)

4.3.8 Drug Release

4.3.8.1 Spectrophotometric Analysis of Model Drug

The solution of IN in MeOH was prepared for a UV-visible spectrophotometer to identify the maximum absorption wavelength. The absorbance at the characteristic peak of IN was used to determine the amount of drug released from the calibration curve.

4.3.8.2 Determination of Drug Content

The IN-loaded DCNR and IN-doped PCz/DCNR films (film area of 3.14 cm^2) were immersed in hexane. The 0.3 mL of each solution was determined a drug content in each component was measured using a UV-visible spectrophotometer at 324 nm. A calibration curve was used to determine amount of the drug in each sample.

4.3.8.3 In Vitro Drug Permeation Study

A modified Franz diffusion cell was used to study the electrically controlled release of the drug from the prepared IN-loaded DCNR films and IN-doped PCz/DCNR blend films at various crosslink ratios (Sittiwong *et al.*, 2012). A PBS buffer solution at a pH of 7.4 was filled in a receptor compartment. The cell was submerged in a water bath to maintain constant temperature at 37 ± 0.5 °C. The film in a donor compartment was placed over a pig's abdominal skin (7 cm^2) above the receptor. Electrical potential was applied through the system by placing a cathode electrode sheet on the film which was connected to a power supply (KETHLEY 1100V Source Meter) at 0-9 V. The amount of drug which diffused through the pig skin to the buffer solution was detected by the UV-visible spectrophotometer.

4.4 Results and discussion

4.4.1 Characterization

4.4.1.1 Crosslink Density of the Crosslinked DCNR Film

The crosslinking process of rubber, under UV irradiator in the presence of a photoinitiator (MMMP) and a crosslinking agent (TMPTMP), started with the interaction between TMPTMP and radicals of MMMP. Sulfide radicals from a crosslinker were formed and then joined rubber molecules together by attacking at allyl groups of rubber structure (Choi *et al.*, 2005).

Figure 4.1 shows the crosslink density of the crosslinked DCNR film under the effect of crosslink ratio. The crosslink density significantly increases with increasing crosslink ratio. Active free radicals of a TMPTMP are more initiated with increasing crosslinking agent concentration, resulting in denser crosslinked rubber chains (Huang *et al.*, 2011) and reduceing the solvent penetration and uptake. The crosslink density is not proportional to a concentration of crosslinker as the crosslink ratio is higher than 0.0056. A higher crosslinked network limits a mobility of active sites in a network (Phinyocheep and Duangthong, 2000) and an entanglement of macroradicals restricts a reaction with a free radical of crosslinker (Rettler *et al.*, 2012).

4.4.1.2 FT-IR Characteristics of IN-doped PCz

The FT-IR spectra of PCz, IN, and IN-doped PCz are shown in Figure 4.2. The FT-IR spectrum of PCz shows the N-H stretching of heteroaromatics peak at 3415 cm^{-1} which is broader than the one of Cz monomer, the C=C stretching of the aromatic compound at 1600-1625 cm^{-1}, the C-N-C stretching peak at 1451 cm^{-1}, the C-H out of plan bending at 1326 cm^{-1}, and the 1,2,4-trisubstitution peaks at 806 cm^{-1}, 855 cm^{-1}, and 884 cm^{-1} (Naddaka *et al.*, 2011, Raj *et al.*, 2010, Taoudi *et al.*, 1997, 2000).

Characteristic peaks of IN are the aromatic C-H stretching at 3021 cm^{1}, the C-H stretching vibrations at 2963 cm^{-1}, the C=O stretching vibrations at 1720 cm^{-1}, the asymmetric aromatic O-C stretching at 1228 cm^{-1}, and symmetric aromatic O-H stretching at 1085 cm^{-1} (Dupeyron *et al.*, 2013).

The FT-IR spectrum of IN-doped PCz is similar to the peak of PCz except the peak at 1287 cm^{-1} which can be refered to the carboxylate group of IN which was used to dope PCz.

4.4.2.3 Thermal Stability of IN-doped PCz

Figure 4.3 shows the decomposition temperature of IN which is 302.05 °C. The decomposition temperature of dedoped PCz displays at 576.02 °C and 741.41 °C due to an elimination of residual dopant (Cl^-) and a decomposition of PCz backbone, respectively (Syed Abthagir *et al.*, 1998). The IN-doped PCz shows the decomposition temperatures at 256.76 °C, 585.60 °C, and 753.79 °C which can be refered to the deformation of IN, residual dopant, and degradation of PCz backbone, respectively. The decomposition temperature of IN-doped PCz confirm the IN doped on the PCz by the ionic interaction between carboxylate group of IN and amine group of PCz as indentified by the FT-IR at 1287 cm^{-1} (Cabaniss and McVey, 1995).

4.4.2 Release Kinetics of Model Drug

4.4.2.1 Determination of Actual Drug Content

The actual amount of IN presented in the IN-loaded DCNR film and IN-doped PCz/DCNR film (film area of 3.14 cm^2) at the crosslink ratio of 0.0008, 0.0032, and 0.0064 were 0.79 ± 0.57, 0.72 ± 0.15, and 0.85 ± 0.11 mg, respectively. While the actual amount of IN in IN-doped PCz/DCNR film (film area of 3.14 cm^2) was 0.71 ± 0.02 mg. The actual amount of IN was reported as the percentage of the initial content of IN-loaded into the films.

4.4.2.2 Release Kinetic of IN from IN-loaded DCNR Film and IN-doped PCz/DCNR Film

The IN release and permeation behaviors of DCNR films were investigated and analyzed based on the Korsmeyer-Peppas model (Korsmeyer *et al.*, 1983), Eq. (4.7):

$$\frac{M_t}{M_\infty} = kt^n \qquad (4.7)$$

where M_t and M_∞ are the amounts of IN released from DCNR film (mg) at time t and the total amount of drug released (mg), respectively, k is the kinetic constant (h^{-n}), t is the release time (h), and n is the diffusion scaling exponent.

The amount of IN released from the DCNR films was also force-fitted with the Higuchi equation (n = 0.5) (Higuchi, 1961) and the diffusion coefficient was calculated from the slope of the plot of the amounts of IN release from the film at time t versus square root of time using Eq. (4.8), Eq. (4.9), and Eq. (4.10):

$$\frac{M_t}{M_\infty} = kt^{1/2} \quad (4.8)$$

$$Q = \frac{M_t}{A} = 2C_0\left(\frac{Dt}{\pi}\right)^{1/2} \quad (4.9)$$

$$M_t = k_H M_\infty t^{1/2} = 2C_0 \left(\frac{D^{1/2}}{\pi^{1/2}}\right) A\, t^{1/2} \quad (4.10)$$

where M_t/M_∞ is the fractional drug released, k_H is the kinetic constant (t^{-n}), t is the release time (h), Q is the amount of material flowing through a unit cross section of barrier (g/cm^2) in unit time, C_0 is the initial drug concentration in the film (g/cm^3), and D is the diffusion coefficient of a drug (cm^2/s)

Table 4.1 shows the n value of IN release and permeation from DCNR films and PCz/DCNR films with and without electric field. There are two stages of n value presented in n_1 and n_2 for the first and second stages, respectively. The n_1 values of DCNR films are varied between 0.322-0.596 and 0.354-0.748 with and without electric field, respectively. While the n_2 values of DCNR films are varied between 1.705-1.772 and 1.216-1.644 with and without electric field, respectively. For all of the n values, the n_1 and n_2 depend on the crosslink ratio and the electric field strength. At the n value less than 0.5 (as shown in n1 value), the drug transport mechanism from film is diffusion controlled called Quasi Fickian diffusion (Pasparakis *et al.*, 2006, Pradhan *et al.*, 2008, Mahmoodi *et al.*, 2010) At the n value between 0.5 and 1 (as shown in n_1 value), the drug transport

behavior is an anomalous transport which occurs from a pure diffusion and a matrix swelling (Lowman and Peppas, 1999). At the n value higher than 1 (as shown in n_2 value), it corresponds to the Super Case II transport in which the drug transport mechanism occurs through a relaxation of polymer and an erosion mechanism (Sriamornsak *et al.*, 2007).

4.4.2.3 Effect of Crosslink Ratio

There is a 3-step process of the IN release and permeation from the IN-loaded DCNR films as shown in Figure 4.4. First, the drug does not diffuse through the films and the pig skin yet. Second, the amount of drug- dramatically increases with time, and finally the third step the system obtains an equilibrium after 56-72 h. The amount of drug permeation increases with decreasing crosslink ratio (24, 17, and 12 % for crosslink ratio of 0.0008, 0.0032, and 0.0064, respectively) as a higher free volume between rubber networks allows drug molecules to penetrate more easily through the film (Paradee *et al.*, 2012).

The diffusion coefficients of IN through DCNR film (Table 1) were calculated from the slopes of the plots in Figure 4.5 using the Higuchi's equation (Eq. (4.8)). There are two stages of diffusion coefficient that are varied between 5.85E-10 8.36E-10 to 1.37E-09cm^2/s and 9.61E-084.39E-07 to 4.39E-07 cm^2/s for the first and second stage, respectively as shown in Table 4.1. The diffusion coefficient decreases with increasing crosslink ratio as a smaller pathway in a denser crosslinked network limiting drug molecules to diffuse through the matrix (Mwangi and Ofner Iii, 2004).

4.4.2.4 Effect of Electric Field Strength

Figure 4.6 shows the amount of IN release and permeation from the DCNR films at 0.0032 crosslink ratio in a period of time t versus the square root of time at various electric field strengths under the cathode (negatively charged electrode) placed on the IN-loaded DCNR film. The amount of IN permeation increases (17-36 % at the E = 0-7 V) with increasing electric field strength resulting from the electrical repulsion between the negatively charged drug and the negatively charged electrode, the so-called electro-repulsive force which was generated at a sufficiently high electric field strength (Sittiwong *et al.*, 2012). In addition, an aqueous pathway (pores) in the bilayer membranes of stratum corneum of pig skin is

expected to be induced by applied electric field. The electric field induced pathway simplifies a transport of the drug through the membranes (Weaver *et al.*, 1999). The diffusion coefficient of IN from DCNR film under applied electric field provides two stages which are 4.49E-09 to 5.55E-08 cm^2/s and 2.32E-07 to 1.42E-06 cm^2/s for the first and second stage, respectively depending on electric field strength as shown in table 4.1. The diffusion coefficient of IN from the DCNR film increases with increasing electric field strength. The drug molecule easily diffuses from the DCNR film due to the electro-repulsive force enhancing the drug mobility (Chansai *et al.*, 2009).

4.4.2.5 Effect of Conductive Polymer

The amount of IN release and permeation from the IN-doped PCz/DCNR film increases (19-58 % at the E = 0-5 V) with increasing electric field strength as shown in Figure 4.7. The electric field induces a greater amount of IN released due to the electro-repulsive force. Furthermore, the electric field also provides a stronger reduction reaction of IN from PCz. The counter ions of drug which were combined on the PCz during the doping process can be released upon applying a negative potential via the reduction reaction (Niamlang and Sirivat, 2009).

Figure 4.8 and 4.9 shows the first and the second stage of diffusion coefficient of IN from the DCNR film and IN-doped PCz/DCNR films at various electric field strengths (E = 0-9 V), respectively. The diffusion coefficients increase with increasing electric field strength because of the higher electro-repulsive force. For the first stage, the diffusion coefficient is not significantly different from each other because a large PCz molecule hinders a drug diffusion pathway. While, the diffusion coefficient in the second stage of IN from the IN-doped PCz/DCNR film is higher than that of DCNR film at the same electric field strength. The erosion of a film promotes a free volume in a matrix, moreover the binding of IN on PCz allow an easier release of the anionic drug as PCz processes higher electrical conductivity than DCNR resulting in a greater response to the electric field in driving IN from the films by the reduction reaction (Miller *et al.*, 1987)

In vitro skin permeation study, the pigskin was placed between IN-loaded DCNR film and receptor medium. Table 4.1 shows the diffusion coefficients of IN from the DCNR films and IN-doped PCz/DCNR films. There are

two stages of diffusion coefficient as 5.38E-10 to 3.81E-08 cm^2/s and 8.01E-07 to 7.12E-06 cm^2/s at E = 0-7 V for the first and second stage, respectively. The diffusion coefficient of the first stage is lower than that of second stage because of pore generation and erosion of the film. The diffusion coefficients of IN increase with decreasing crosslink ratio as drug molecules are less entrapped in a matrix with a lower crosslinks than that with a higher crosslinks (Mwangi and Ofner Iii, 2004). Moreover, the diffusion coefficient is higher under applied electric field because of the electro-repulsive force. (Chansai *et al.*, 2009). The diffusion efficient is the highest under using PCz as the drug carrier and blended with DCNR film as PCz provides the reduction reaction between IN and PCz under applied electric field (Niamlang and Sirivat, 2009). Pongjanyakul *et al.* (2003) studied and obtained the diffusion of nicotine from acrylic rubber as 0.35×10^{-8} cm^2/s to 1.09×10^{-8} cm^2/s depending on the ratio of nicotine to acrylic acid. The diffusion coefficient of nicotine is higher than that of the first stage of IN from the DCNR films without the electric field (5.85E-10 to 1.37E-09 cm^2/s) because of the size of nicotine (8.2 Angstrom) smaller than IN (13.9 Angstrom). However, the diffusion coefficient of IN under applied the electric field is higher due to the electro-repulsive force from electric field. Juntanon *et al.* (2007) investigated the effect of electric field on the permeation of sulfosalicylic acid (SSA) from poly(vinyl alcohol) (PVA) hydrogels. The diffusion coefficient of SSA from PVA without applied electric field (0.29E-9 to 2.08E-09 cm^2/s) is higher than that of IN from DCNR film because the PVA consists of pore size which promotes the drug diffusion. Furthermore, the size of SSA (9.25 Angstrom) is smaller than IN that facilitate the drug diffusion from the matrix. The diffusion coefficient of SSA at electric field of 1 V varied from 7.42E-09 to 1.97E-09cm^2/s which is lower than that of IN (4.86E-09 cm^2/s at E = 1 V) at the crosslinking ratio of 0.5-5.0. However, the diffusion coefficient of SSA from uncrosslinked PVA is higher than that of IN at E = 1 V because of larger mesh size. the The diffusion coefficient in the first stage of IN from PCz/DCNR blend film at the same electric field strength is higher than that of sulfosalicylic acid from the PVA hydrogels due to the reduction reaction of PCz as a conductive polymer under electric field. In addition, the diffusion coefficient of IN in the second stage is higher than that of nicotine and SSA all case. In the second stage of IN permeation, the

DCNR film creates pore via DCNR film erosion which promote the IN transport and IN diffusion.

Thus, the diffusion behavior of the drug through the polymer matrix can be affected by many factors including the chemical composition of the drug, the molecular weight and size of drug, the interaction between drug and matrix, the matrix, and the experimental set up (Juntanon *et al.*, 2007).

4.4.2.6 Release and Permeation Time

A plot of amount of IN permeated from the film versus square root of time can be divided time into three regions. In the first region, the amount of IN permeation is independent a square root of time so called the permeation time (t_P). The permeation time occurred from a nature of the NR matrix which affected to a delay of IN permeation. The second region, IN permeated through the film by diffusion phenomenon into a PBS buffer which provided an increasing amount of IN permeation as a function of time, the so called the release duration1 (t_{R1}). For the third region, IN permeated via an erosion of the matrix as so called the release duration2 (t_{R2}). As shown in Table 4.2, the permeation time increases from 6.31 to 7.56 h with increasing crosslink ratio from 0.0008 to 0.0032 because of the denser network (Paradee *et al.*, 2012). For the effect of an electric field on IN-loaded DCNR film, the permeation time decreases with increasing electric field strength due to the electrorepulsive force and the pore expansion at 5 V of electric field strength. The permeation time of IN permeated from the PCz/DCNR blend film was lower than that from DCNR film with applying electric field because of electro-repulsive force. While the permeation time of IN from the blend film was higher than one from the DCNR film at E = 0 V because of the steric hindrance between the IN molecules and PCz backbones. Considering the release duration1 and the release duration2, the release time1 of IN permeated from the DCNR film decreased with increasing either the crosslink ratio or electric field strength resulting from the film was decayed at the same time and initially generated the release duration2. While the release duration2 of IN permeated from PCz/DCNR blend film obviously decreased with increasing electric field strength; it took a shorter time to reach its equilibrium amount of IN permeation relative to other conditions.

4.4.3 Pore Morphology of the Film after the Permeation Study

Figure 4.10 shows the morphology of IN-loaded DCNR films before and after the release and permeation study with and without the electric field. Before the release and permeation study, SEM images show a smooth surface of the film without a porous appearance. The pores were then generated on surface of the DCNR films after the release and permeation study, consistent with a previous study (Soulas *et al.*, 2012). In an absence of an electric field, a surface showed quite irregular pore surfaces , whereas for the film with electric field showed a highly dispersed pores throughout the surface (Pichayakorn *et al.*, 2012).

Considering on pore size over a polymer matrix surface after the release and permeation study (Table 4.3), the IN-loaded DCNR films at the crosslink ratio of 0.0032 provides the pore sizes of 19.64 ± 15.95 and 1.29 ± 0.37 μm under electric field of 0 and 3 V, respectively. For the IN-doped PCz/DCNR films at the same crosslink ratio, the pore sizes are 20.78 ± 7.25, 3.60 ± 1.69, 2.91 ± 1.34, 90.71 ± 30.00, and 102.49 ± 66.68 μm under electric field strengths of 0, 1, 3, 5, and 7 V, respectively. The pore sizes are nearly the same for the two systems without electric field. Moreover, pore sizes on the films varied a great deal under an absence of electric field, providing a wide pore size distribution. For the films under applied electric field, the pore size increased with electric field strength which can be directly related to the increases in the amount of IN permeation and the diffusion coefficient.

For the DCNR film with and without an electric field, the pore was slightly generated on the surface of the film due to the DCNR surface degradation. Thus, the permeation time of IN from IN-loaded DCNR film at 0 and 3 V electric field strengths can be associated with the pore generation (Table 4.2 and Figure 4.11). The results convincingly suggest that the pores were created mainly by the permeation of IN through the film matrix into the PBS buffer. For the permeation and release study of IN-loaded DCNR film under an electric field, the pore area to film area ratio reached an equilibrium faster than the one without an electric field as shown in Figure 4.11, which can be related to the larger amount of IN permeation under applied electric field. In summary, our results clearly indicate that the amount of IN molecules released and permeated through the rubber matrix and pig skin critically depends on the polymer matrix, crosslink density, the penetrant, and electric field (George and Thomas, 2001 and Juntanon *et al.*, 2008).

4.5 Conclusions

The IN-loaded DCNR films and the IN-doped PCz/DCNR blend films were investigated for the release and permeation mechanism behavior and the diffusion coefficient of the drug under the effects of crosslink ratio and electric field strength. The crosslink density obtained by a swelling method showed a decrease of the density of rubber network with increasing crosslink ratio as a denser network reduced a solvent penetration and uptake. The diffusion coefficients of IN through the films were acquired by the force-fitted plots of the amounts of IN released versus time to the Higuchi's equation under the effect of crosslink ratio, electric field strength, and conductive polymer. The diffusion coefficients of the drug through the DCNR films decreased with increasing crosslink ratio resulting from the denser networks. For the effect of the electric field strength, the diffusion coefficient of the drug from the DCNR films was directly influenced by the strength of an applied electric field due to the electro repulsive interaction between the negatively charged drug and the negatively charged electrode. In addition, IN released from the PCz/DCNR blend films exhibited a higher diffusion coefficient than one from the DCNR films due to the reduction reaction of the conductive polymer which promoted a delivery of the drug through the membranes. Thus, the PCz/DCNR film is shown here as a potential candidate for the transdermal patch used under applied electric field.

4.6 Acknowledgements

This work is financially supported by the Conductive and Electroactive Polymer Research Unit; the Thailand Research Fund (TRF-RTA); The Royal Thai Government; and The Petroleum and Petrochemical College, Chulalongkorn University.

4.7 References

Al Minnath, M., Unnikrishnan, G., Purushothaman, E., 2011. Transport studies of thermoplastic polyurethane/natural rubber (TPU/NR) blends. J. Membr. Sci. 379(1-2), 361-369.

Cabaniss, S.E., McVey, I.F., 1995. Aqueous infrared carboxylate absorbances: aliphatic monocarboxylates. Spectrochim. Acta Mol. Biomol. Spectros. 51(13), 2385-2395.

Chansai, P., Anuvat, S., Niamlang, S., Chotpattananont, D., Viravaidya-Pasuwat, K., 2009. Controlled transdermal iontophoresis of sulfosalicylic acid from polypyrrole/poly(acrylic acid) hydrogel. Int. J. Pharm. 381(1), 25-33.

Choi, S.S., Hong, J.P., Seo, Y.S., Chung, S.M., Nah, C., 2006. Fabrication and characterization of electrospun polybutadiene fibers crosslinked by UV irradiation. J. Appl. Polym. Sci. 101(4), 2333-2337.

Chou, H.-W., Huang, J.-S., 2008. Effects of ultraviolet irradiation on the static and dynamic properties of neoprene rubbers. J. Appl. Polym. Sci. 110(5), 2907-2913.

Debjit Bhowmik, C., Chiranjib ,Chandira, M., Jayakar, B., Sampath, K.P. 2010. Recent advances in transdermal drug delivery system. Int. J. PharmTech. Research. 2(1), 68-77

Dupeyron, D., Kawakami, M., Ferreira, A.M., Caceres-Velez, P.R., Rieumont, J., Azevedo, R.B., Carvalho, J.C., 2013. Design of indomethacin-loaded nanoparticles: effect of polymer matrix and surfactant. Int. J. Nanomedicine. 8, 3467-3477.

George, S.C., Thomas, S., 2001. Transport phenomena through polymeric systems. Prog. Polym. Sci. 26(6), 985-1017.

Gupta, B., and Prakash, R., 2010. Interfacial polymerization of carbazole: Morphology controlled synthesis. Synth. Met. 160(5-6), 523-528.

Herculano, R.D., Guimarães, S.A.C., Belmonte, G.C., Duarte, M.A., Hungaro Oliveira Júnior, O.N., Kinoshita, A., Graeff, C.F.O., 2010. Metronidazole release using natural rubber latex as matrix. Materials Research. 13, 57-61.

Higuchi, T. 1961. Rate of release of medicaments from ointment bases containing drugs in suspension. J. Pharm. Sci. 50(10), 874-875.

Huang, X., Li, C., Zhu, W., Zhang, D., Guan G., Xiao, Y., 2011. Ultraviolet-induced crosslinking of poly(butylene succinate) and its thermal property, dynamic mechanical property, and biodegradability. Polym. Adv. Technol. 22(5), 648-656.

Juntanon, K., Niamlang, S., Rujiravanit, R., Sirivat, A., 2008. Electrically controlled release of sulfosalicylic acid from crosslinked poly(vinyl alcohol) hydrogel. Int. J. Pharm. 356(1-2), 1-11.

Korsmeyer, R. W., Gurny, R., Doelker, E., Buri, P., Peppas, N.A., 1983. Mechanisms of solute release from porous hydrophilic polymers. Int. J. Pharm. 15(1), 25-35.

Lowman, A.M., Peppas, N.A., 1999. Hydrogels. Encyclopedia of controlled drug delivery. 1, 397-418.

Mahmoodi, M., Khosroshahi, M.E., Atyabi, F., 2010. Laser thrombolysis and in vitro study of tPA release encapsulated by chitosan coated PLGA nanoparticles for AMI. Int J Biol Biomed Eng. 4,35-42.

Miller, L.L., Zinger, B., Zhou, Q.X., 1987. Electrically controlled release of hexacyanoferrate($^{4-}$) from polypyrrole. J. Am. Chem. Soc. 109(8), 2267-2272.

Morin, J.-F., Leclerc, M., Adès, D., Siove, A., 2005. Polycarbazoles: 25 years of progress. Macromol. Rapid Commun. 26(10), 761-778.

Mwangi, J.W., Ofner Iii, C.M., 2004. Crosslinked gelatin matrices: release of a random coil macromolecular solute. Int. J. Pharm. 278(2), 319-327.

Naddaka, M., Mondal, E., Lellouche, J.-P., 2011. Oxidative fabrication of spherical polycarbazole-based microparticles. Mater. Lett. 65(8), 1165-1167.

Niamlang, S., Sirivat, A., 2009. Electrically controlled release of salicylic acid from poly(p-phenylene vinylene)/polyacrylamide hydrogels. Int. J. Pharm. 371(1-2), 126-133.

Paradee, N., Sirivat, A., Niamlang, S., Prissanaroon-Ouajai, W., 2012. Effects of crosslinking ratio, model drugs, and electric field strength on electrically controlled release for alginate-based hydrogel. J. Mater. Sci. 23, 999-1010.

Pasparakis,G., Bouropoulos, N., 2006. Swelling studied and in vitro release of verapamil from calcium alginate and calcium alginate-chitosan beads. Int. J. Pharm. 3323, 34-42.

Phinyocheep, P., Duangthong S., 2000. Ultraviolet-curable liquid natural rubber. J. Appl. Polym. Sci. 78(8), 1478-1485.

Pichayakorn, W., Suksaeree, J., Boonme, P., Amnuaikit, T., Taweepreda, W., Ritthidej, G.C., 2012. Nicotine transdermal patches using polymeric natural rubber as the matrix controlling system: Effect of polymer and plasticizer blends. J. Membr. Sci. 411-412(0), 81-90.

Pongjanyakul, T., Prakongpan, S., Priprem, A., 2003. Acrylic matrix type nicotine transdermal patches: in vitro evaluations and batch-to-batch uniformity. Drug Dev. Ind. Pharm. 29(8), 843-853.

Pradhan, R., Budhathoki, U., Thapa, P., 2008. Formulation of once a day controlled release tablet of indomethacin based on HPMC-man-nitol. MUSET. 1, 55-67.

Prausnitz, M.R., and Langer, R., 2008. Transdermal drug delivery. Nat. Biotechnol. 26(11), 1261-1268.

Raj, V., Madheswari, D., Mubarak Ali, M., 2010. Chemical formation, characterization and properties of polycarbazole. J. Appl. Polym. Sci. 116(1), 147-154.

Rettler, E.F.J., Rudolph, T., Hanisch, A., Hoeppener, S., Retsch, M., Schubert, U.S., Schacher, F.H., 2012. UV-induced crosslinking of the polybutadiene domains in lamellar polystyrene-block-polybutadiene block copolymer films – An in-depth study. Polymer. 53(25), 5641-5648.

Sittiwong, J., Niamlang, S., Paradee, N., Sirivat, A., 2012. Electric field-controlled benzoic acid and sulphanilamide delivery from poly(vinyl alcohol) hydrogel. J. AAPS. 13(4), 1407-1415.

Soulas, D.N., Papadokostaki, K.G., 2011. Regulation of proxyphylline's release from silicone rubber matrices by the use of osmotically active excipients and a multi-layer system. Int. J. Pharm. 408(1-2), 120-129.

Soulas, D.N., Sanopoulou, M., Papadokostaki, K.G., 2012. Proxyphylline release kinetics from symmetrical three-layer silicone rubber matrices: Effect of

different excipients in the outer rate-controlling layers. Int. J. Pharm. 427(2), 192-200.

Sriamornsak, P., Thirawong, N., Korkerd, K., 2007. Swelling, erosion and release behavior of alginate-based matrix tablets. Eur. J. Pharm. Biopharm. 66(3), 435-450.

Syed Abthagir, P., Dhanalakshmi, K., Saraswathi, R., 1998. Thermal studies on polyindole and polycarbazole. Synth. Met. 93(1), 1-7.

Taoudi, H., Bernede, J.C., Bonnet, A., Morsli, M., Godoy, A., 1997. Comparison of polycarbazole obtained by oxidation of carbazole either in solution or in thin film form. Thin Solid Films. 304(1-2), 48-55.

Taoudi, H., Bernede, J.C., Del Valle, M.A., Bonnet, A., Molinie, P., Morsli, M., Diaz, F., Tregouet, Y., Bareau. A., 2000. Polycarbazole obtained by electrochemical polymerization of monomers either in solution or in thin film form. J. Appl. Polym. Sci. 75(13), 1561-1568.

Uhrich, K.E., Cannizzaro, S.M., Langer, R.S., Shakesheff, K.M., 1999. Polymeric Systems for Controlled Drug Release. Chem. Rev. 99(11), 3181-3198.

Weaver, J.C., Vaughan, T.E., Chizmadzhev, Y., 1999. Theory of electrical creation of aqueous pathways across skin transport barriers. Adv. Drug Deliv. Rev. 35(1), 21-39.

Table 4.1 Comparison of diffusion coefficient and kinetic factor of drug permeated from different matrix (continued)

Matrix	Drug size (°A)	Power law			Higuchi		D (cm^2/s)	E (V)	Remarks
		n_2	$10^2 k_2$ (h^{-n})	r^2	$10^2 k_{H2}$ (h^{-n})	r^2			
Natural rubber	13.9[c]	1.772	8.71E-04	0.981	0.17	0.954	4.39E-07	0	Crosslink ratio = 0.0008
		1.705	1.28E-03	0.989	0.11	0.951	2.11E-07		Crosslink ratio = 0.0032
		1.755	9.79E-04	0.993	0.08	0.932	9.61E-08		Crosslink ratio = 0.0064
		1.476	2.84E-03	0.993	0.11	0.952	2.32E-07	0.1	Crosslink ratio = 0.0032
		1.216	5.70E-03	0.953	0.17	0.933	5.46E-07	1	
		1.644	1.41E-03	0.989	0.18	0.322	6.32E-07	3	
		1.407	4.14E-03	0.993	0.23	0.985	1.00E-06	5	
		1.438	3.39E-03	0.994	0.25	0.976	1.19E-06	7	
		1.615	1.85E-03	0.995	0.27	0.985	1.42E-06	9	
Polycarbazole/Natural rubber, (PCz/NR)		2.736	2.23E-05	0.994	0.20	0.933	8.01E-07	0	Crosslink ratio = 0.0032
		2.515	6.73E-05	0.991	0.33	0.941	2.14E-06	1	
		2.183	1.95E-04	0.994	0.39	0.945	3.00E-06	3	
		3.116	6.95E-06	0.943	0.60	0.968	7.11E-06	5	
		2.591	4.72E-05	0.981	0.60	0.967	7.12E-06	7	

Table 4.1 Comparison of diffusion coefficient and kinetic factor of drug permeated from different matrix (continued)

Matrix	Drug size (°A)	Power law			Higuchi		D (cm^2/s)	E (V)	Remarks
		n	10^2 k (h^{-n})	r^2	10^2 k_H (h^{-n})	r^2			
Acrylic rubber[a]	8.2[d]	-	-	-	37.61	-	0.35E-8	0	Nicotine (1.10g): Acrylic (34.36g)
		-	-	-	49.32	-	0.34E-8		Nicotine (1.50g): Acrylic (33.64g)
		-	-	-	71.11	-	0.36E-8		Nicotine (2.00g): Acrylic (32.73g)
		-	-	-	257.41	-	1.09E-8		Nicotine (4.00g): Acrylic (29.09g)
Poly(vinyl alcohol), (PVA)[b]	9.25[c]	0.58	-	-	13.13	0.990	2.08E-9	0	Uncrosslink
		0.72	-	-	9.54	0.985	1.08E-9		Crosslink ratio = 0.5
		0.77	-	-	11.17	0.845	0.51E-9		Crosslink ratio = 2.5
		0.82	-	-	6.72	0.896	0.29E-9		Crosslink ratio = 5.0
		0.63	-	-	11.97	0.984	7.42E-9	1	Uncrosslink
		0.83	-	-	7.08	0.983	4.62E-9		Crosslink ratio = 0.5
		0.93	-	-	5.49	0.972	2.90E-9		Crosslink ratio = 2.5
		0.93	-	-	4.29	0.947	1.97E-9		Crosslink ratio = 5.0

[a] Pongjanyakul *et al.* (2003)

[b] Juntanon *et al.* (2007)

[c] Indomethacin in PBS buffer (pH 7.4), 37 °C

[d] Nicotine in PBS buffer (pH 7.4), 37 °C

[e] Sulfosalicylic acid in acetate buffer (pH 5.5), 37 °C

Table 4.2 Permeation and release time of IN permeated from IN-loaded DCNR films and PCz/DCNR blend films

Matrix	E (V)	CL	Permeation time (h)	Release time 1 (h)	Release time 2 (h)	Release and permeation time (h)
NR	0	0.0008	6.31	20.52	35.88	56.40
NR	0	0.0032	6.89	13.18	43.67	56.85
NR	0	0.0064	7.56	12.16	43.50	55.65
NR	0.1	0.0032	9.08	11.80	45.20	57.00
NR	1	0.0032	9.36	13.68	42.87	56.55
NR	3	0.0032	7.46	14.63	42.67	57.30
NR	5	0.0032	2.99	18.54	40.29	58.83
NR	7	0.0032	0.50	18.42	37.53	55.95
NR	9	0.0032	0.23	18.87	38.13	57.00
PCz/NR	0	0.0032	11.29	16.59	38.17	54.76
PCz/NR	1	0.0032	6.25	17.66	38.89	56.55
PCz/NR	3	0.0032	2.28	20.00	36.25	56.25
PCz/NR	5	0.0032	0.42	21.86	33.20	55.06
PCz/NR	7	0.0032	0.36	21.64	33.57	55.20

Table 4.3 Pore size on a surface of IN-loaded DCNR films and IN-doped PCz/DCNR films after the permeation study

Matrix	Crosslink ratio (mol $_{TMPTMP}$/mol $_{isoprene}$)	Electric field (V)	Pore size (μm)
NR	0.0032	0	19.64 ± 15.95
NR	0.0032	3	1.29 ± 0.37
NR	0.0064	3	14.69 ± 12.80
PCz/NR	0.0032	0	20.78 ± 7.25
PCz/NR	0.0032	1	3.60 ± 1.69
PCz/NR	0.0032	3	2.91 ± 1.34
PCz/NR	0.0032	5	90.71 ± 30.00
PCz/NR	0.0032	7	102.49 ± 66.68

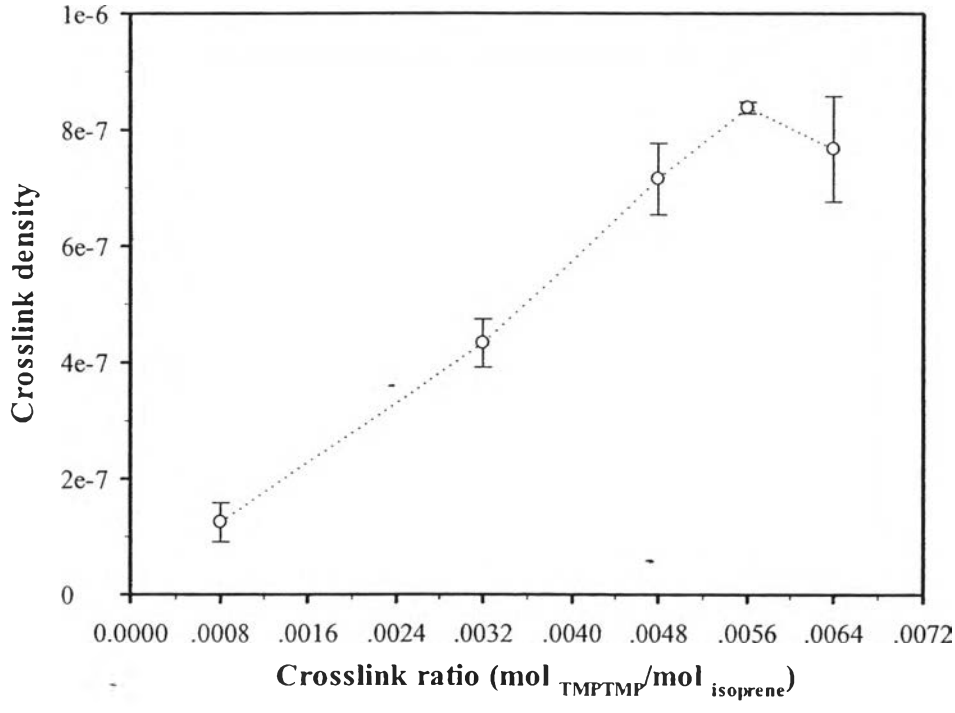

Figure 4.1 Crosslink density of crosslinked DCNR film with various crosslink ratios.

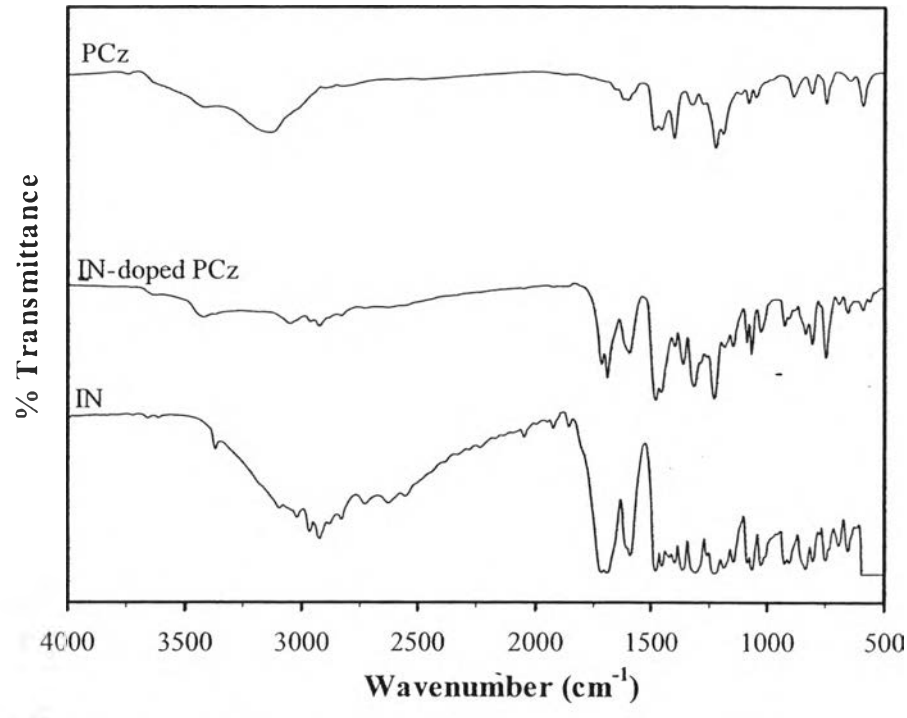

Figure 4.2 FT-IR spectrum of: a) PCz; b) IN; and c) IN-doped PCz.

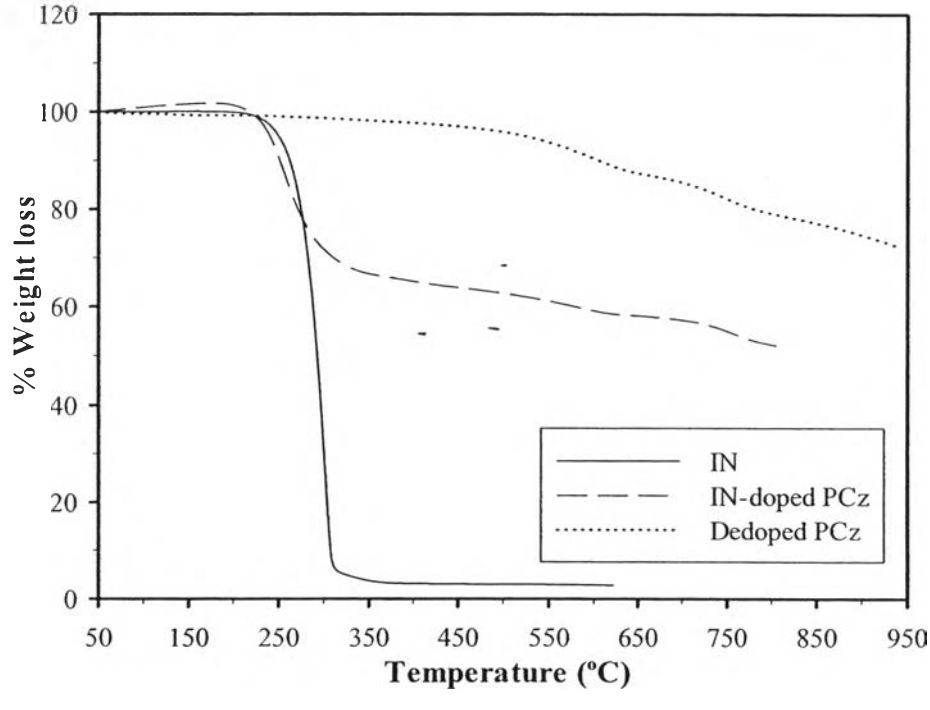

Figure 4.3 TGA thermograms of: a) dedoped PCz; b) IN; and c) IN-doped PCz.

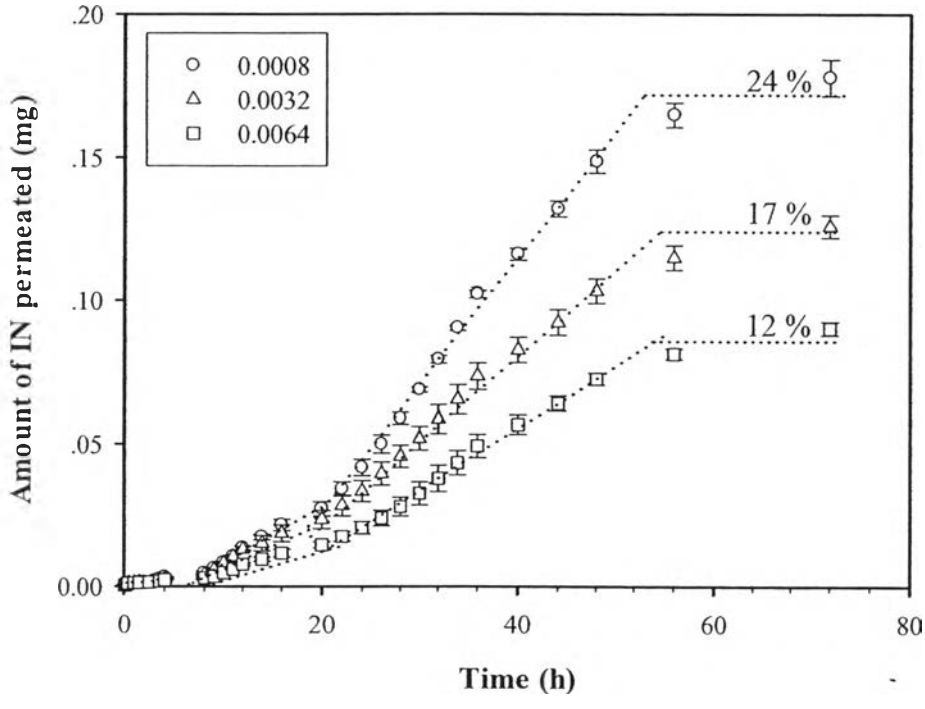

Figure 4.4 Amount of IN permeated from crosslinked DCNR film with various crosslink ratios ($mol_{TMPTMP}/mol_{isoprene}$) versus time t under absence of electric field, pH 7.4, 37 °C.

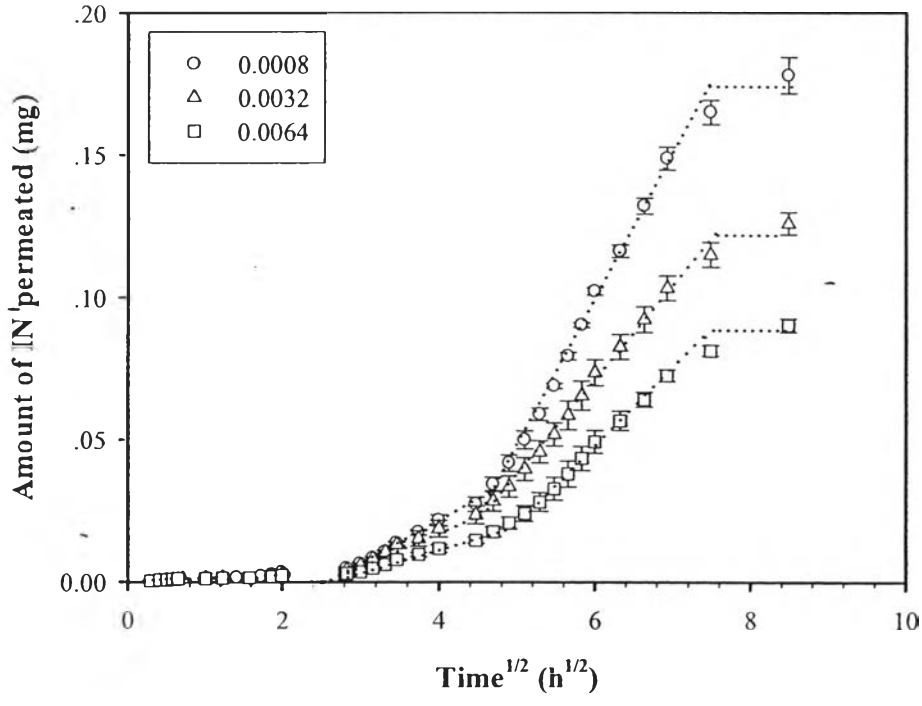

Figure 4.5 Amounts of IN permeated from IN-loaded DCNR films versus time$^{1/2}$ with various crosslink ratios ($mol_{TMPTMP}/mol_{isoprene}$) under absence of electric field, pH 7.4, 37 °C.

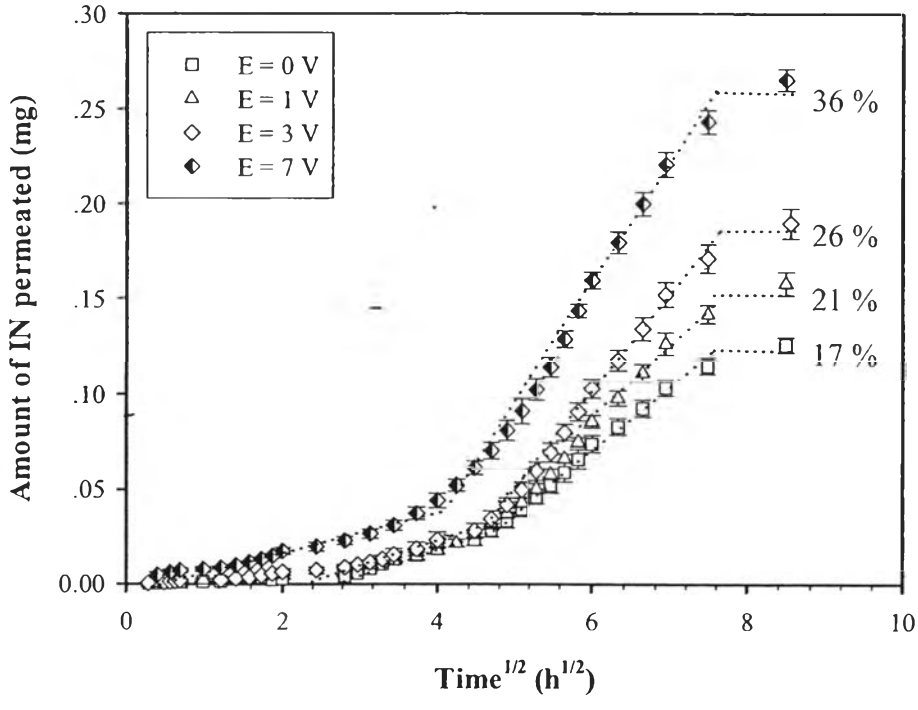

Figure 4.6 Amounts of IN permeated from IN-loaded DCNR films versus time$^{1/2}$ at various electric field strengths, at 0.0032 crosslink ratio, pH 7.4, 37 °C.

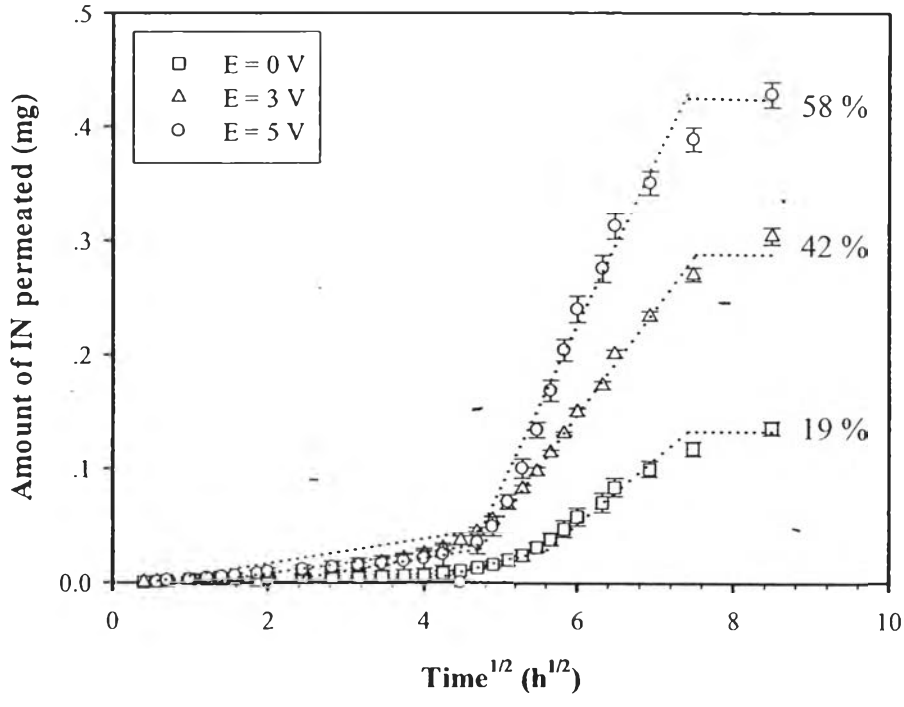

Figure 4.7 Amounts of IN permeated from IN-doped PCz/DCNR films versus time$^{1/2}$ at various electric field strengths, at 0.0032 crosslink ratio, pH 7.4, 37 °C.

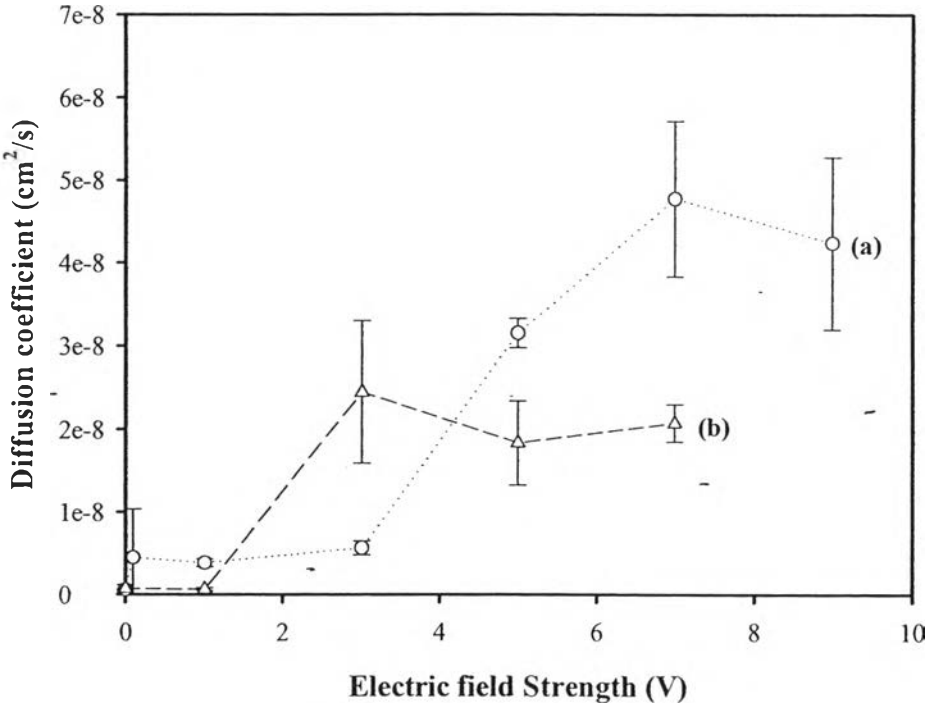

Figure 4.8 Diffusion coefficients (n_I) of IN permeated from IN-loaded DCNR film (a) and IN-doped PCz/DCNR film (b) versus $time^{1/2}$ at various electric field strengths, at 0.0032 crosslink ratio, pH 7.4, 37 °C.

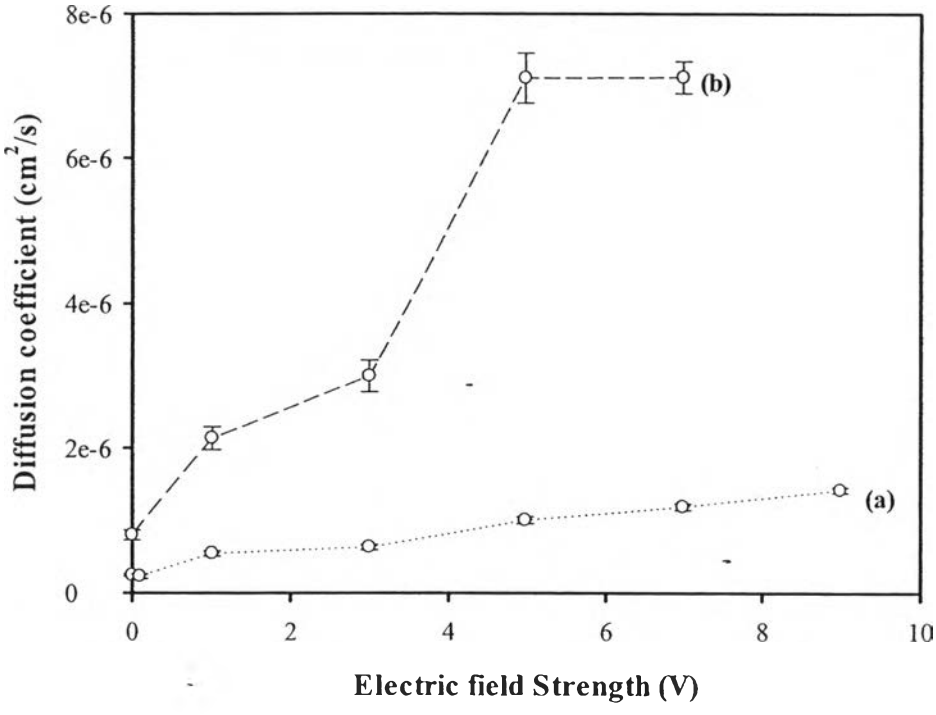

Figure 4.9 Diffusion coefficients (n_2) of IN permeated from IN-loaded DCNR film (a) and IN-doped PCz/DCNR film (b) versus time$^{1/2}$ at various electric field strengths, at 0.0032 crosslink ratio, pH 7.4, 37 °C.

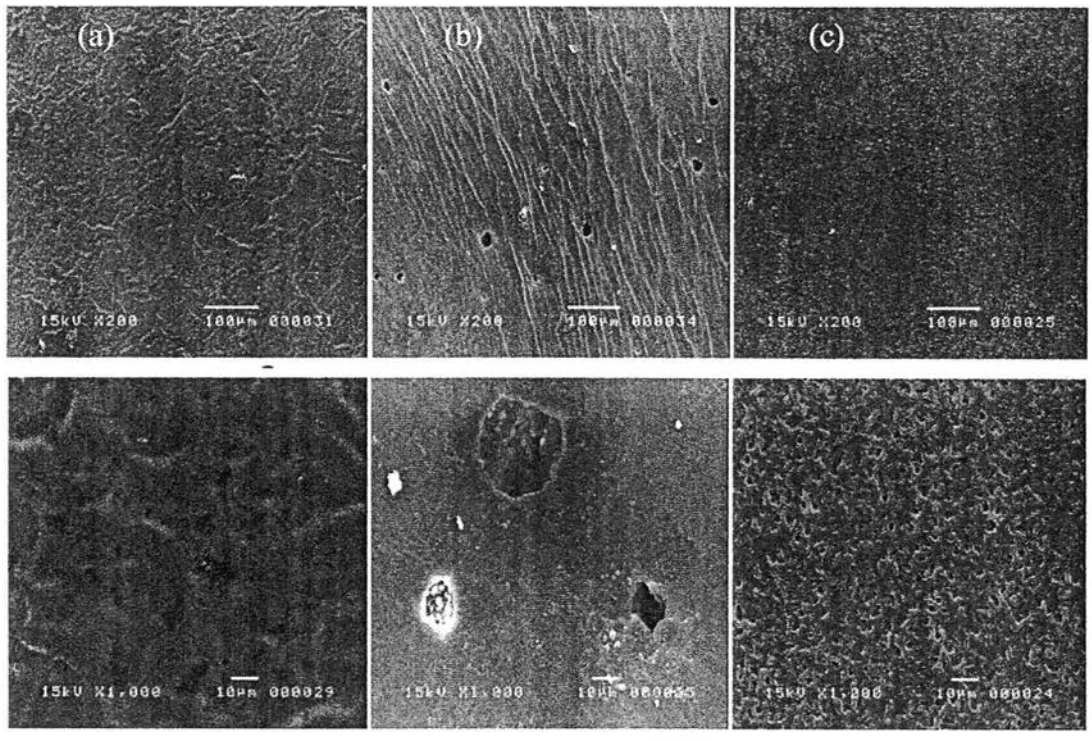

Figure 4.10 SEM micrographs of crosslinked DCNR film at 0.0032 crosslink ratio: (a) before the permeation study; (b) after the permeation study without electric field; and (c) after the permeation study under electric field in PBS buffer pH 7.4 at 200 and 1k of magnification.

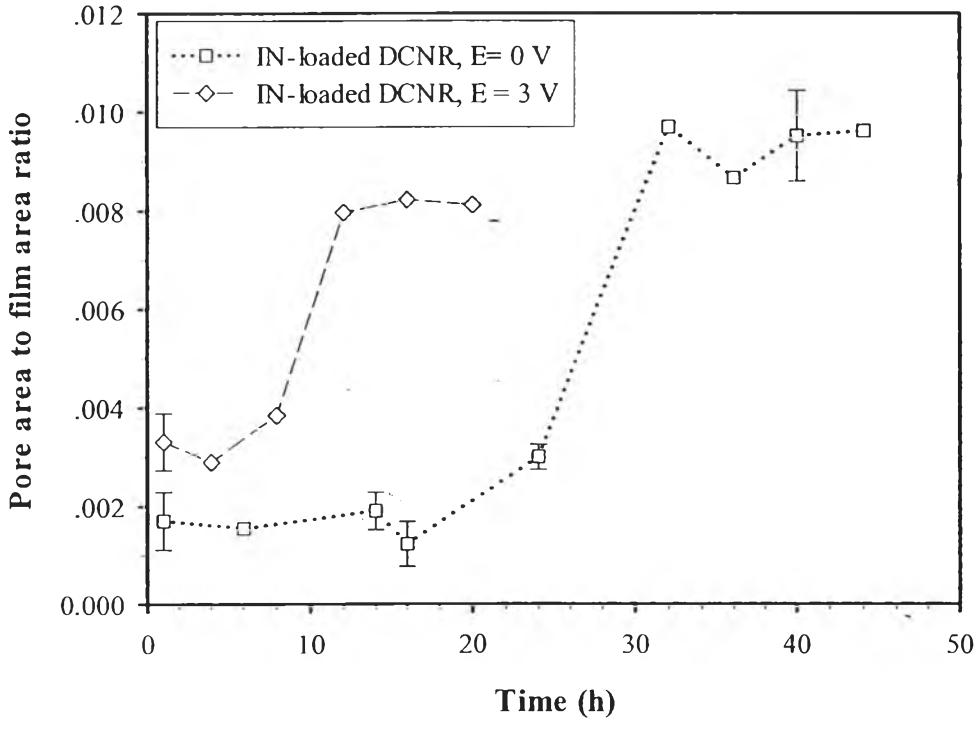

Figure 4.11 Pore area to film area ratio of IN-loaded DCNR films as a function of time under 0 and 3 V of the electric field strengths.